



Climatic and Tectonic Forcing Lead to Contrasting Headwater Slope Evolutions

Yinbing Zhu¹, Patrice Rey¹, Tristan Salles¹

¹School of Geosciences, University of Sydney, Sydney, NSW, 2006, Australia

5 *Correspondence to:* Patrice F. Rey (patrice.rey@sydney.edu.au)

Abstract. Landscapes evolve through the coupled effects of tectonics and surface processes. Previous studies have shown that uplift rate changes generate upstream-migrating erosion waves, altering downstream slopes while upstream ones remain constant until the wave arrives. However, the distinctive differences between landscape responses to uplift versus climatic changes, particularly rainfall rate changes, remain incompletely described. This study uses a numerical model to investigate
10 landscape responses to changes in both rainfall and uplift rates. Results show that, unlike the simple upstream-migrating erosion waves from uplift rate changes, rainfall rate changes generate more complex responses. Specifically, rainfall rate changes cause transient slope change reversals at the headwaters due to differential erosion between the divide and its adjacent areas, a pattern not observed in uplift-induced evolution. These reversals are more pronounced when hillslope diffusion plays a dominant role (i.e., high diffusion coefficient). While both tectonic and climatic forcing drive landscape
15 change, they produce recognizably different signatures in river profiles. If these distinctive signatures can be identified from river profiles or inferred from erosion rate measurements, they can help disentangle climatic and tectonic influences on landscape evolution.

1 Introduction

Whilst tectonic and geodynamic forces generate longer wavelength topography, Earth's surface processes powered by
20 climate dissect the Earth's surface, creating high-frequency topographic features that contribute to the reconfiguration of drainage patterns and the re-routing of sediments from source to sink (e.g., Allen, 2008; Wobus et al., 2006a; Whipple et al., 2013; Martinsen et al., 2022; Seybold et al., 2021). Whether or not climatic and tectonic disturbances impact landscape evolution differently has been debated for decades (e.g., Kirby and Whipple, 2012; Whipple, 2009; Bonnet and Crave, 2003; Whittaker, 2012). Previous research has focused on various landscape features, such as river channels, drainage divide, and
25 alluvial fans, to understand whether or not they respond differently to tectonic and climatic disturbances (Leonard and Whipple, 2021; Mao et al., 2021; Shi et al., 2021; Willett et al., 2014). Rivers, in particular, have been found to respond strongly to climatic and tectonic disturbances, making them a valuable feature for studying how landscapes evolve (Molin et al., 2023; Quye-Sawyer et al., 2021; D'arcy and Whittaker, 2014). Here, we investigate via numerical experiments how river channels respond to climatic and uplift disturbances, paying particular attention to the role of hillslope diffusion, which is



30 often overlooked in favour of river incision processes. We show that river channels respond slightly differently to tectonic and climatic changes when hillslope diffusion is considered. After changes in uplift rate, the channel slope at the headwaters records a monotonic increase (uplift rate increase) or decrease (uplift rate decrease). In contrast, after changes in rainfall rate, the channel slope records a non-monotonic adjustment, which becomes more pronounced as the surface diffusion coefficient increases. We suggest that changes in rainfall rate cause a transient spatial variation in erosion rate around the divide area
35 due to the interaction between hillslope diffusion and river incision. This difference has the potential to distinguish between tectonic and climatic influences on landscape evolution.

1.1 River incision vs hillslope diffusion

Several numerical models have been proposed to quantify river incision processes (e.g., Dietrich et al., 2003; Howard and Kerby, 1983; Perron et al., 2008). The most commonly used is the detachment-limited stream power model, which assumes
40 that sediments are instantly flushed from the channel and that the bedrock erosion rate E depends on the channel slope S , drainage area A , and precipitation P :

$$E = k_d (PA)^m S^n \quad (1)$$

where m and n are positive constant exponents, and k_d is a coefficient describing the erodibility of the channel bed and reflects the combined impacts on the erosion of climate, lithology, bedload, and other potential parameters (Kirby and
45 Whipple, 2012; Smith et al., 2022; Whipple and Tucker, 1999). Following the principle of conservation of mass, the rate of surface elevation change ($\partial z / \partial t$) is determined by the difference between the uplift rate U and erosion rate:

$$\frac{\partial z}{\partial t} = U - E \quad (2)$$

As rivers incise, the sloping ground at their flanks increases, driving hillslope diffusion, which describes the downward transport of creeping soil (Fernandes and Dietrich, 1997; Dietrich et al., 2003). Models indicate that the convexity of the
50 hillslope profile is influenced by hillslope processes and the rate of incision at the hillslope base (e.g., Armstrong, 1987; Ahnert, 1987). Hence, river incision and hillslope diffusion are coupled and evolve simultaneously. A simple model describing the process of hillslope diffusion assumes that the flux of soil along hillslopes is linearly related to the hillslope gradient (e.g., Culling, 1963, 1960; Salles and Duclaux, 2014; Tucker and Hancock, 2010):

$$\frac{\partial z}{\partial t} = k_{hl} \nabla^2 z \quad (3)$$

55 where k_{hl} is the hillslope diffusion coefficient, which integrates climate, lithology, soil conditions, and biotic influences (Dietrich and Perron, 2006; Hurst et al., 2013; Robl et al., 2017). Hillslope diffusion gradually transports soil and sediment downslope due to gravity and reshapes substantially the landscape over time (e.g., Litwin et al., 2024; Perron et al., 2008; Roering, 2008). It has been shown that hillslope diffusion strongly influences drainage density and valley spacing (Perron et al., 2008; Sweeney et al., 2015; Tucker and Bras, 1998). Additionally, the sediment and soil transported from hillslopes
60 impact river incision by either acting as tools for erosion or forming a protective cover that shields the underlying bedrock from further erosion (Sklar and Dietrich, 2001).



While much research has focused on river channel evolution (e.g., Kirby and Whipple, 2012; Wobus et al., 2010), few have explored whether and how river channels respond differently to tectonic and climatic changes when hillslope diffusion is included. Before addressing this issue, the following paragraph clarifies the notions of steady-state and transient landscapes.

65 1.2 Steady state vs transient landscapes

Computer-generated landscapes evolving under controlled tectonic and climatic conditions provide a robust framework for better understanding the formation and evolution of natural landscapes (e.g., Chen et al., 2014; Pan et al., 2021; Salles and Hardiman, 2016; Schwanghart and Scherler, 2014). These models show that a landscape reaches a steady state when the uplift rate equals the erosion rate. When the uplift rate changes, landscapes are in a transient state of disequilibrium and evolve to reach a new steady state (e.g., Leonard and Whipple, 2021; Miller et al., 2012; O'hara et al., 2019). Steady-state and transient landscapes show a sharp contrast in the variation of rivers' profiles. When a river channel has reached a steady state, its longitudinal elevation profile is usually smooth and concave-up (Fig. 1a). In contrast, under uniform lithology, knickpoints form in transient river channels (Wobus et al., 2006b; Lague, 2014; Neely et al., 2017; Whipple et al., 2013). A knickpoint is a location where there is an abrupt change in the channel slope (Fig. 1b). A positive knickpoint forms where the slope suddenly increases downstream, while a negative knickpoint forms where the slope decreases abruptly. A mobile positive knickpoint indicates an increase in uplift rate and/or a decrease in erosion efficiency (induced by a decrease in rainfall rate, for example), while a mobile negative knickpoint indicates the opposite conditions (Baldwin et al., 2003). Both types of knickpoints typically form at the river mouth and migrate upstream toward the headwaters.

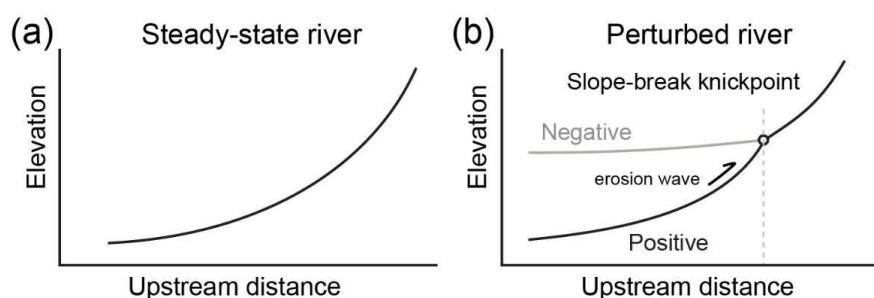


Figure 1. Channel profiles with different morphology. (a) a steady-state river profile. (b) Transient river profiles with a negative or positive slope-break knickpoint.

A migrating knickpoint separates the channel into two segments, upstream and downstream segments. It has been proposed that regardless of whether the transient change is driven by tectonics or climate, the elevation of the upstream segment changes while its slope remains constant. After the downstream segment reaches a steady state, its channel elevation and slope have changed (e.g., Whipple, 2001; Whipple and Tucker, 1999).



2 Methodology and model setup

To investigate landscape evolution under climatic or tectonic changes, as well as varying erodibility and hillslope diffusion, we use the long-term surface evolution model Badlands (Basin and Landscape Dynamics) (Salles, 2016; Salles and Hardiman, 2016). Badlands is designed to simulate i/ landscape development via the mobilisation of sediments through hillslope diffusion and stream-power incision, ii/ sediment transport from source to sink and into marine environments, iii/ sediment accumulation in sedimentary basins, and iv/ isostatic re-adjustment of Earth's lithosphere due to surface loading and unloading. Although nonlinear diffusion models may better describe sediment transport on hillslopes (e.g., Jiménez-Hornero et al., 2005; Martin, 2000; Roering et al., 1999), for simplicity, our model assumes that hillslope sediment transport rates are linearly proportional to the slope gradient. Here, we explore landscape responses to changes in rainfall or uplift, and we disregard isostatic re-adjustment. In particular, we focus on contrasts in drainage network patterns, contrasts in average elevation, contrasts in surface roughness, and contrasts in river profiles.

Our initial landscape models are mapped over a 40 km × 80 km grid with a uniform initial elevation of 10 m and a spatial resolution of 400 m × 400 m. We design four initial models with varying hillslope diffusion and erodibility coefficients (Table 1). The diffusion coefficient is set to 0 in model M1, meaning the landscape evolution is purely driven by riverine processes with an erodibility coefficient of $2.3 \times 10^{-6} \text{ yr}^{-1}$. We set the diffusion coefficient to 1 m²/yr in model M2 and 2 m²/yr in model M3. Finally, in our last model M4, the erodibility is doubled to $4.6 \times 10^{-6} \text{ yr}^{-1}$.

Table 1. Diffusion coefficient and erodibility of four models

Model	Diffusion coefficient k_{hl} (m ² /yr)	Erodibility k_d (1/yr)
M1	0	2.3×10^{-6}
M2	1	2.3×10^{-6}
M3	2	2.3×10^{-6}
M4	2	4.6×10^{-6}

Our four models are submitted to a combination of uniform uplift at a rate of 300 m/Myr and background rainfall at a rate of 2 m/yr until they reach a steady state equilibrium, where mean elevation and river profiles no longer change (Montgomery, 2001; Willett & Brandon, 2002). This first stage lasts for 25 Myr (Fig. 2), after which all models reach a steady state.

In the second stage, which also lasts 25 Myr, each model is subjected to a perturbation while the other forcing remains constant. We either:

- Increase rainfall to 6 m/yr or decrease it to 0.67 m/yr, while keeping uplift fixed at 300 m/Myr, or
- Increase uplift to 900 m/Myr or decrease it to 100 m/Myr, while keeping rainfall fixed at 2 m/yr.



This design yields 16 individual experiments (Fig. 2), allowing us to assess landscape responses to changes in rainfall and uplift rates separately.

115

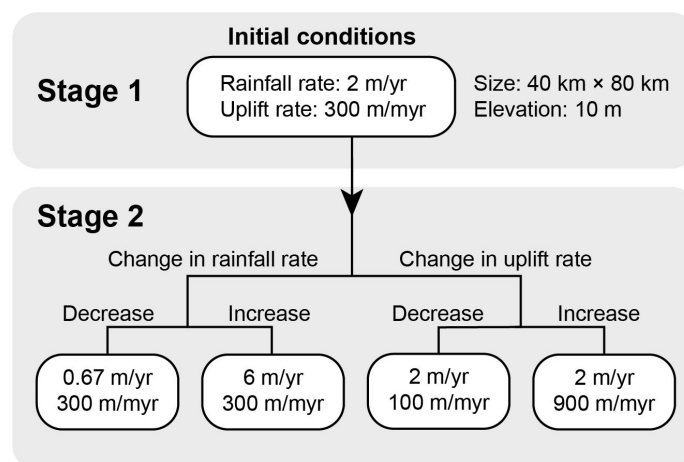


Figure 2. Each of our four initial models (M1 to M4) experiences four different two-stage landscape evolutions controlled by changes in rainfall or uplift. Stage 1: An initial flat landscape is uplifted under an uplift rate of 300 m/Myr and a rainfall rate of 2 m/yr until a steady-state landscape is reached. Stage 2: Changes in rainfall or uplift rate.

120 3 Results

3.1 Comparison of final, steady-state landscapes

Impact on patterns of drainage networks: Despite having different erosion and diffusion coefficients and going through different climatic and tectonic histories, our four initial models display broadly similar patterns of drainage networks. In all 16 cases, the two largest drainage basins form at the eastern and western parts of the landscape, separated by a central divide (Fig. 3). Interestingly, the drainage patterns in models M2 and M4 are highly similar, reflecting that both models have the same ratio of hillslope diffusion to erodibility.

125

Impact on average elevation and surface roughness: Our results show that the mean landscape elevation and surface roughness increase following a decrease in rainfall rate or an increase in uplift rate and decrease following an increase in rainfall rate or a decrease in uplift rate. Regardless of rainfall or uplift changes, the absence of hillslope diffusion in M1 ($k_{hl} = 0$) leads to the largest surface roughness (Fig. 3a). When hillslope diffusion is included, the landscapes in models M2, M3, and M4 are smoother than those in model M1 (Fig. 3b-d). Models M2 and M4 show that, regardless of rainfall or uplift changes, doubling both the diffusion and erosion coefficients reduces both the mean elevation and the mean surface roughness by a factor of ~2. Interestingly, models M2 and M3 show that doubling only the diffusion coefficient reduces the

130



surface roughness by ~15% and, surprisingly, increases the mean elevation by ~20%. Models M3 and M4 show that
135 doubling the erosion coefficient alone reduces the mean elevation by a factor of more than 2.

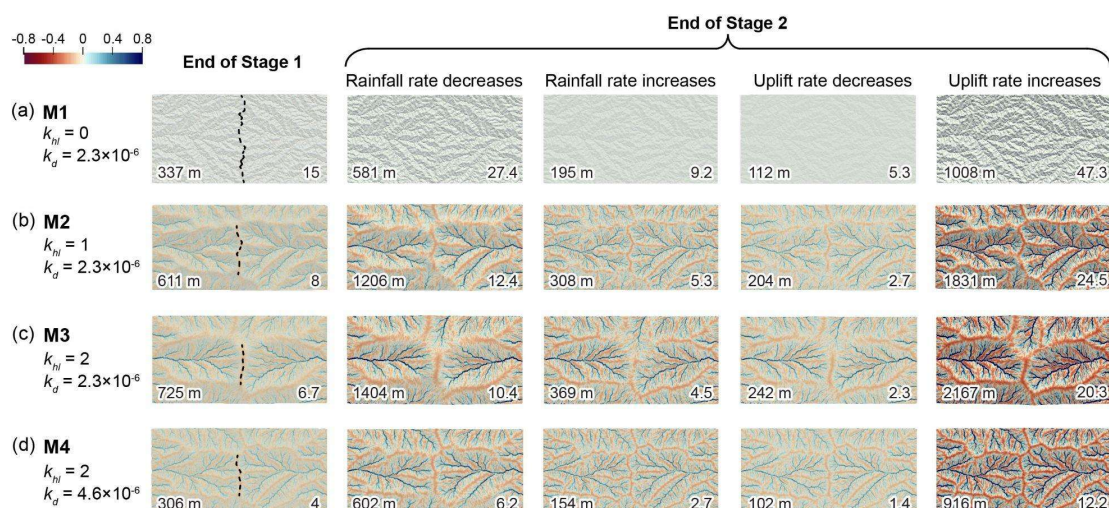


Figure 3. Hillshade maps showing erosion and deposition rates resulting from hillslope diffusion at the end of Stage 1 and the end of Stage 2 for models M1 (a), M2 (b), M3 (c), and M4 (d). Each model differs in hillslope diffusion coefficients (k_{hl}) and erodibility values (k_d). Blue areas indicate deposition, while red areas represent erosion. Color bar values indicate depositional (positive) and erosional (negative) rates (mm/yr). Numbers at the bottom left of each map display the mean elevation, while numbers at the bottom right display the mean surface roughness, calculated using the ‘roughness’ algorithm of GDAL in QGIS (Wilson et al., 2007). Dashed lines on maps at the end of Stage 1 denote the divides. The divides in Stage 2 are similar to those in Stage 1 and are not marked in this stage.

3.2 Impact on rivers’ channel response

To explore channel responses to changes in rainfall or uplift rates under various ratios of hillslope diffusion to erodibility, we analyze the trunk stream of the western basin, including the evolution of erosion and deposition, as well as the evolution of the longitudinal channel profile. Although we present results only from the western basin, we have verified that both
150 drainage basins exhibit similar evolutions. Given the overall consistency in river channel behavior across all models, we present the results from model M1 (no hillslope diffusion), highlighting the key differences observed in models M2 to M4 (all with non-zero hillslope diffusion).

After a decrease in rainfall rate or an increase in uplift rate, the trunk stream is uplifted with the increase in landscape elevation and the channel slope. A positive knickpoint and an erosion wave develop, migrating upstream from the river
155 mouth (Fig. 4a and d). The downstream channel first reaches a steady state, with no further changes in elevation and slope. The entire channel returns to a new steady state once the erosion wave reaches the headwaters and the knickpoint disappears.



Conversely, an increase in rainfall rate or a decrease in uplift rate lowers the channel elevation and its slope, creating a negative knickpoint at the river mouth and an erosion wave that migrates upstream (Fig. 4b and c). Once the erosion wave reaches the headwaters, the channel eventually reaches a steady state.

160

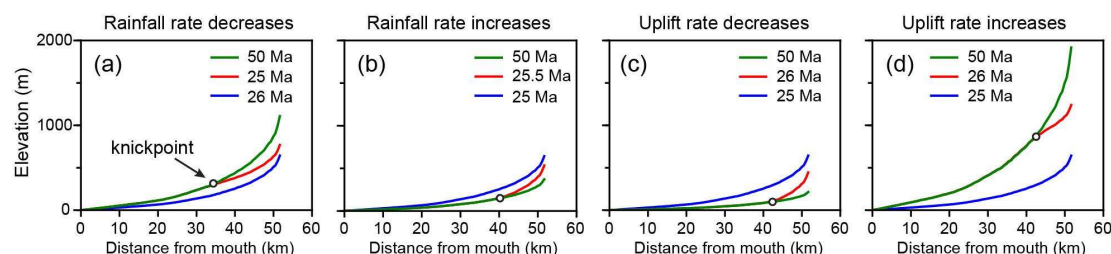
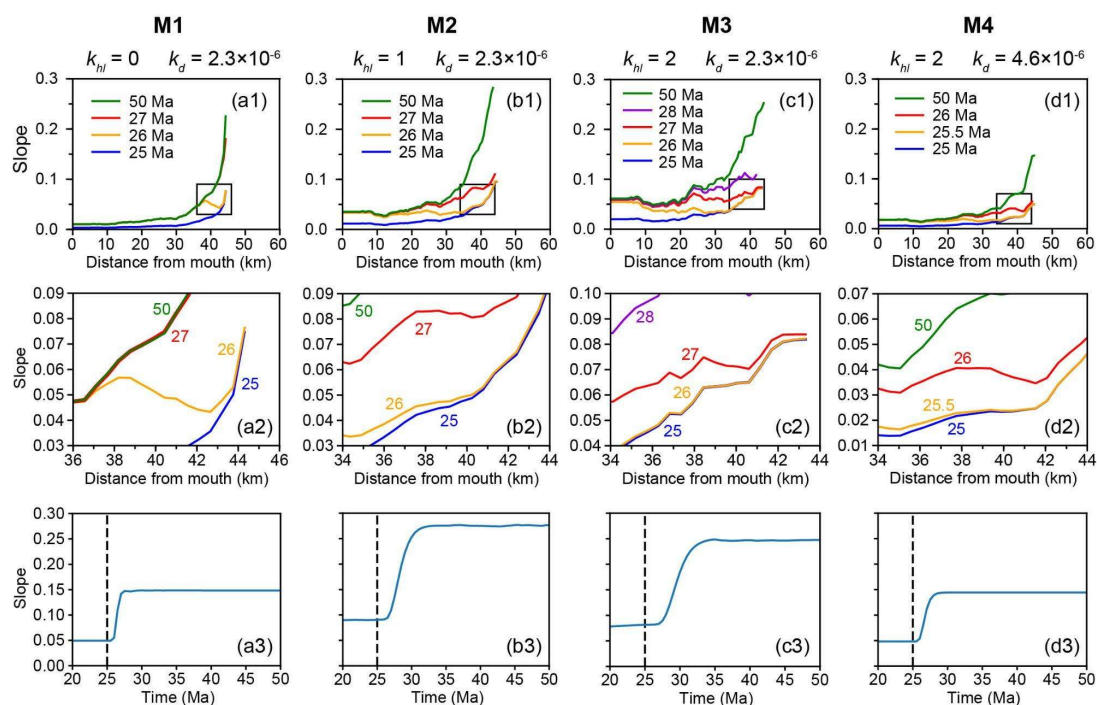


Figure 4. Longitudinal profiles of the trunk stream after changes in rainfall or uplift rates in model M1. The changes occur at 25 Ma, affecting the steady state trunk stream in blue.

165 When the hillslope diffusion is absent (model M1), the slope of the trunk stream headwaters remains nearly constant for 1-2 Myrs following a change in either uplift or rainfall rate (Fig. 5 a1-3 and Fig. 6 a1-3). The slope then increases monotonously after the arrival of the upstream migrating erosion wave (Whipple and Tucker, 1999).



170 **Figure 5. Evolution of trunk stream slope following an increase in uplift rate. (a1-d1) Longitudinal slope profiles of the trunk stream at selected time steps (colored lines), with each subplot corresponding to a model (M1-M4). Black rectangles indicate the headwater regions. (a2-d2) Enlarged views of the headwater areas, corresponding to the boxed regions in (a1-d1). (a3-d3) Temporal evolution of the mean channel slope in the upper ~800 m of the trunk stream, capturing the dynamic slope response across model runs. Dashed vertical lines mark the timing of the uplift rate increase (25 Ma).**

175

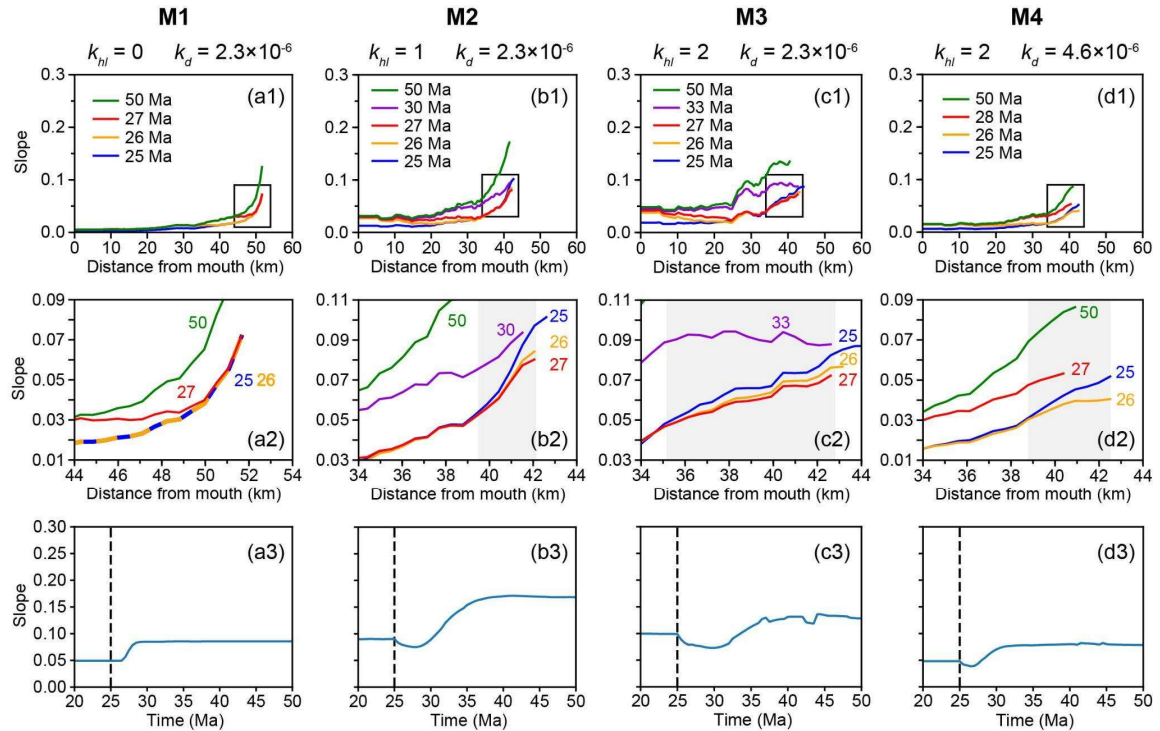


Figure 6. Evolution of trunk stream slope following a decrease in rainfall rate. (a1-d1) Longitudinal slope profiles of the trunk stream at selected time steps (colored lines), with each subplot corresponding to a model (M1-M4). Black rectangles indicate the headwater regions. (a2-d2) Enlarged views of the headwater areas, corresponding to the boxed regions in (a1-d1). Grey bands indicate the regions where the transient slope change reversal occurs. (a3-d3) Temporal evolution of the mean channel slope in the upper ~800 m of the trunk stream, capturing the dynamic slope response across model runs. Dashed vertical lines mark the timing of the rainfall rate decrease (25 Ma).

In contrast, when hillslope diffusion is present (models M2, M3, and M4), we observe major differences in the evolution of river headwater slopes following changes in uplift and rainfall rates. An increase in uplift rate leads to a monotonic slope increase in the headwaters (Fig. 5 b1-3, c1-3, and d1-3). In contrast, a decrease in rainfall rate first leads to a transient slope decrease, followed by a subsequent increase, a phenomenon we refer to as “*transient slope change reversal*” (Fig. 6 b1-3, c1-3, and d1-3). The opposite pattern occurs when the rainfall rate increases: a temporary slope increase is followed by a decrease. Interestingly, we find that transient slope change reversals are associated with hillslope diffusion and river incision.

In model 3, which has the largest ratio of diffusion coefficient to erodibility, longer channels experience transient slope change reversals (Fig. 6 c2), and transient slope change reversals persist longer in time than in the other models (Fig. 6 c3).

In contrast, when hillslope diffusion is present (models M2, M3, and M4), we observe major differences in the evolution of river headwater slopes following changes in uplift and rainfall rates. An increase in uplift rate leads to a monotonic slope



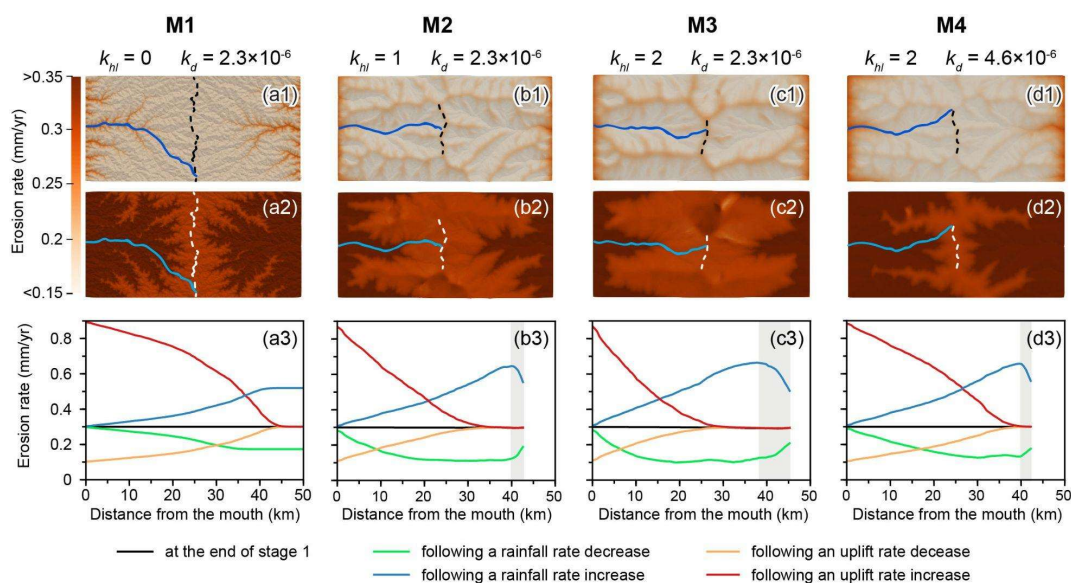
increase in the headwaters (Fig. 5 b1-3, c1-3, and d1-3). In contrast, a decrease in rainfall rate first leads to a transient slope decrease, followed by a subsequent increase, a phenomenon we refer to as “*transient slope change reversal*” (Fig. 6 b1-3, c1-3, and d1-3). The opposite pattern occurs when the rainfall rate increases: a temporary slope increase is followed by a decrease. Interestingly, we find that transient slope change reversals are associated with hillslope diffusion and river incision. In model M3, which has the largest ratio of diffusion coefficient to erodibility, longer channels experience transient slope change reversals (Fig. 6 c2), and transient slope change reversals persist longer in time than in the other models (Fig. 6 c3).

4 Discussion

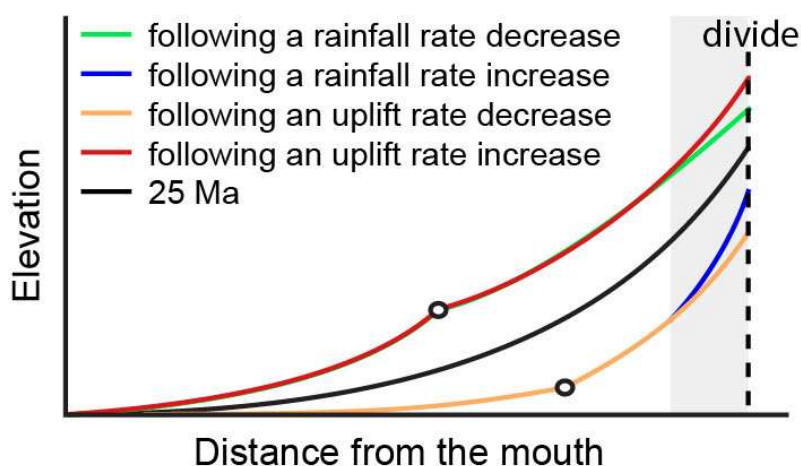
To better understand the cause of the transient slope change reversal, we calculate the erosion rate for each grid cell 1 Myr after the disturbance and extract the erosion rate along the trunk stream for all models (Fig. 7). The transient slope change reversal is driven by differential erosion rates between the divide and adjacent areas.

In model M1, the erosion rates of the divide and its adjacent areas remain homogeneous following changes in rainfall and uplift rates (Fig. 7 a3). Similarly, in models M2, M3, and M4, an increase or decrease in uplift rate results in consistent erosion rates between the divide and adjacent areas (red and orange profiles in Fig. 7 b3, c3, and d3). The surface uplift rate is defined as the difference between the uplift and erosion rates. Given the spatial uniformity of uplift rates, equal erosion rates at the divide and its adjacent areas result in identical surface uplift rates, preventing transient slope change reversals (black and red profiles in Fig. 8).

In contrast, following a decrease in rainfall rate in models M2, M3, and M4, the erosion rate of the divide exceeds that of adjacent downstream areas (green profiles in Fig. 7 b3, c3, and d3). This difference in erosion rate directly causes the surface uplift rate of the divide to be lower than that of adjacent downstream areas, resulting in a temporary decrease in the channel slope at the divide and, therefore, triggering a transient slope change reversal (green profile in Fig. 8). Conversely, following an increase in rainfall rate, the erosion rate of the divide is lower than in adjacent areas (blue profiles in Fig. 7 b3, c3, and d3), causing a temporary slope increase at the divide and again triggering a transient slope change reversal (blue profile in Fig. 8). These findings suggest that rainfall changes distinctly influence divide erosion patterns, with spatial contrasts in erosion rate playing a key role in driving transient slope responses.



220 **Figure 7.** Erosion rates (mm/yr) per grid cell, calculated over 1 Myr following (a1-d1) a decrease in rainfall rate and (a2-d2) an increase in uplift rate. Blue lines in (a1-d1) and (a2-d2) represent trunk streams, and dashed lines mark divides. (a3-d3) Longitudinal erosion profiles along trunk streams, with grey bands indicating the regions where the transient slope change reversal occurs.



225

Figure 8. Schematic diagram of the longitudinal profile of the channel in a steady state (black line) or a transient state after changes in rainfall or uplift rate. The grey band indicates the region where the transient slope change reversal occurs.



Therefore, the interaction between hillslope diffusion and river incision is critical in understanding transient slope change reversal. When the rainfall rate changes, the erosion rate throughout the channel is altered, leading to channel adjustment. However, hillslope response lags behind channel response (Clubb et al., 2019), as hillslope diffusion continues transporting materials downstream at the same rate as before the rainfall rate change. While river valleys are heavily influenced by incision, divides are dominated by hillslope diffusion (Dietrich et al., 2003).

Notably, increasing the hillslope diffusion coefficient results in smoother and wider divides and extends the channel length affected by transient slope change reversals (Fig. 7 b3 and c3). In contrast, increasing the erodibility of bedrock enhances river incision. It weakens the diffusion influence on channel evolution, resulting in a narrower divide and a shorter channel reach where the transient slope change reversal occurs (Fig. 7 c3 and d3).

In summary, the transient slope change reversal results from the competition between incision and diffusion following a change in rainfall. This reversal disappears as the erosion wave gradually approaches the divide area, and the landscape returns to a steady state where the erosion rate is spatially uniform.

Transient slope change reversals could be identified using slope-area analysis or χ analysis. Both methods rely on the stream power model, which describes the relationship between channel slope and drainage area as a power function (Flint, 1974). For a river channel in a steady state, plotting log slope against log area yields a straight line. However, in cases of transient slope change reversals, this relationship may deviate from linearity. While slope-area analysis can be sensitive to data noise (e.g., DEM inaccuracies), χ analysis reduces this influence through an integral approach (Royden and Taylor Perron, 2013; Perron and Royden, 2013). For steady-state rivers, χ should also correlate linearly with elevation, whereas nonlinear χ -elevation relationships may indicate transient slope change reversals.

Transient slope change reversals could also be identified by investigating the erosion rate. One approach to quantify erosion rates is using cosmogenic nuclides, particularly radionuclides like ^{10}Be and ^{26}Al (e.g., Balco et al., 2008; Gosse and Phillips, 2001; Lal, 1991; Muzikar, 2009). These nuclides are produced in surface minerals by cosmic ray interactions, with production rates decreasing exponentially with depth due to cosmic ray attenuation (Dunai, 2010; Lal, 1991). Cosmogenic nuclide concentrations increase as a surface remains exposed to cosmic rays (Ivy-Ochs and Kober, 2008). In contrast, in rapidly eroding areas, nuclide concentrations remain low due to the continuous removal of surface materials.

By mapping nuclide concentrations, spatial patterns in erosion rates could be linked to rainfall or uplift changes. For instance, if the erosion rate is relatively uniform around the divide area, it may suggest a transient response driven by tectonic events. Conversely, if nuclide data indicate increasing erosion at the divide while upstream erosion rates decline, a recent decrease in rainfall rate may be involved in the landscape evolution. Thus, cosmogenic nuclide measurements provide a valuable tool to distinguish between climatic and tectonic drivers of landscape change.



5 Conclusion

260 Changes in rainfall and uplift rates induce different responses in the channel slope at the headwaters, with hillslope diffusion playing a crucial role in adjusting these processes. When the rainfall rate changes, hillslope diffusion interacts with river incision to generate transient spatial variations in erosion around the divide area, leading to transient slope change reversals at the headwaters. In contrast, changes in uplift rates result in spatially uniform erosion across the divide area, preventing such reversals. Identifying these reversals from river profiles or erosion rate estimates at different locations could help
265 determine the driving force behind landscape adjustments. A high hillslope diffusion coefficient increases both the duration and spatial extent of these reversals along the river profile. In contrast, higher erodibility enhances river incision and diminishes the role of diffusion, reducing these reversal effects.

Our findings provide new insights into how climatic and tectonic forcing reshape landscapes over time. By investigating the interaction between diffusion and incision, we show that the transient variations in channel profiles, particularly near the
270 divide, provide potential markers for interpreting past landscape evolution and deciphering the complex interplay between tectonic uplift and climatic variability.

Code and data availability. Version 2.2.0 of Badlands used for the landscape and sedimentary evolution modeling is preserved at <https://doi.org/10.5281/zenodo.1069573> (Salles & Howson, 2017), available via GNU General Public License
275 v3.0 and developed openly at <https://github.com/badlands-model/badlands>.

Author contributions. YZ designed and ran the simulations, analyzed the results, and wrote the manuscript. PR contributed to the result analysis and manuscript revision. TS developed the model code and contributed to the manuscript revision.

280 **Competing interests.** The authors declare that they have no conflict of interest.

Acknowledgments. The first author gratefully acknowledges the financial support from the China Scholarship Council (CSC) and the School of Geosciences at the University of Sydney.

References

- 285 Ahnert, F.: Approaches to dynamic equilibrium in theoretical simulations of slope development, *Earth Surface Processes and Landforms*, 12, 3-15, <https://doi.org/10.1002/esp.3290120103>, 1987.
Allen, P. A.: Time scales of tectonic landscapes and their sediment routing systems, Geological Society, London, Special Publications, 296, 7-28, <https://doi.org/10.1144/sp296.2>, 2008.
Armstrong, A. C.: Slopes, boundary conditions, and the development of convexo-concave forms—some numerical
290 experiments, *Earth Surface Processes and Landforms*, 12, 17-30, <https://doi.org/10.1002/esp.3290120104>, 1987.



- Balco, G., Stone, J. O., Lifton, N. A., and Dunai, T. J.: A complete and easily accessible means of calculating surface exposure ages or erosion rates from ^{10}Be and ^{26}Al measurements, *Quaternary Geochronology*, 3, 174-195, <https://doi.org/10.1016/j.quageo.2007.12.001>, 2008.
- Baldwin, J. A., Whipple, K. X., and Tucker, G. E.: Implications of the shear stress river incision model for the timescale of postorogenic decay of topography, *Journal of Geophysical Research: Solid Earth*, 108, <https://doi.org/10.1029/2001jb000550>, 2003.
- Bonnet, S. and Crave, A.: Landscape response to climate change: Insights from experimental modeling and implications for tectonic versus climatic uplift of topography, *Geology*, 31, 123, [https://doi.org/10.1130/0091-7613\(2003\)031<0123:lrteci>2.0.co;2](https://doi.org/10.1130/0091-7613(2003)031<0123:lrteci>2.0.co;2), 2003.
- Chen, A., Darbon, J., and Morel, J.-M.: Landscape evolution models: A review of their fundamental equations, *Geomorphology*, 219, 68-86, <https://doi.org/10.1016/j.geomorph.2014.04.037>, 2014.
- Clubb, F. J., Mudd, S. M., Hurst, M. D., and Grieve, S. W. D.: Differences in channel and hillslope geometry record a migrating uplift wave at the Mendocino triple junction, California, USA, *Geology*, 48, 184-188, <https://doi.org/10.1130/g46939.1>, 2019.
- Culling, W. E. H.: Analytical Theory of Erosion, *The Journal of Geology*, 68, 336-344, <https://doi.org/10.1086/626663>, 1960.
- Culling, W. E. H.: Soil Creep and the Development of Hillside Slopes, *The Journal of Geology*, 71, 127-161, <https://doi.org/10.1086/626891>, 1963.
- D'Arcy, M. and Whittaker, A. C.: Geomorphic constraints on landscape sensitivity to climate in tectonically active areas, *Geomorphology*, 204, 366-381, <https://doi.org/10.1016/j.geomorph.2013.08.019>, 2014.
- Dietrich, W. E. and Perron, J. T.: The search for a topographic signature of life, *Nature*, 439, 411-418, <https://doi.org/10.1038/nature04452>, 2006.
- Dietrich, W. E., Bellugi, D. G., Sklar, L. S., Stock, J. D., Heimsath, A. M., and Roering, J. J.: Geomorphic Transport Laws for Predicting Landscape form and Dynamics, in: *Prediction in Geomorphology*, 103-132, <https://doi.org/https://doi.org/10.1029/135GM09>, 2003.
- Dunai, T. J.: *Cosmogenic nuclides: principles, concepts and applications in the earth surface sciences*, Cambridge University Press, 2010.
- Fernandes, N. F. and Dietrich, W. E.: Hillslope evolution by diffusive processes: The timescale for equilibrium adjustments, *Water Resources Research*, 33, 1307-1318, <https://doi.org/10.1029/97wr00534>, 1997.
- Flint, J.-J.: Stream gradient as a function of order, magnitude, and discharge, *Water Resources Research*, 10, 969-973, <https://doi.org/10.1029/WR010i005p00969>, 1974.
- Gosse, J. C. and Phillips, F. M.: Terrestrial in situ cosmogenic nuclides: theory and application, *Quaternary Science Reviews*, 20, 1475-1560, [https://doi.org/10.1016/s0277-3791\(00\)00171-2](https://doi.org/10.1016/s0277-3791(00)00171-2), 2001.
- Howard, A. D. and Kerby, G.: Channel changes in badlands, *Geological Society of America Bulletin*, 94, 739-752, [https://doi.org/10.1130/0016-7606\(1983\)94<739:CCIB>2.0.CO;2](https://doi.org/10.1130/0016-7606(1983)94<739:CCIB>2.0.CO;2), 1983.
- Hurst, M. D., Mudd, S. M., Attal, M., and Hilley, G.: Hillslopes record the growth and decay of landscapes, *Science*, 341, 868-871, <https://doi.org/10.1126/science.1241791>, 2013.
- Ivy-Ochs, S. and Kober, F.: Surface exposure dating with cosmogenic nuclides, *E&G Quaternary Science Journal*, 57, 179-209, <https://doi.org/10.3285/eg.57.1-2.7>, 2008.
- Jiménez-Hornero, F. J., Laguna, A., and Giráldez, J. V.: Evaluation of linear and nonlinear sediment transport equations using hillslope morphology, *Catena*, 64, 272-280, <https://doi.org/10.1016/j.catena.2005.09.001>, 2005.
- Kirby, E. and Whipple, K. X.: Expression of active tectonics in erosional landscapes, *Journal of Structural Geology*, 44, 54-75, <https://doi.org/10.1016/j.jsg.2012.07.009>, 2012.
- Lague, D.: The stream power river incision model: evidence, theory and beyond, *Earth Surface Processes and Landforms*, 39, 38-61, <https://doi.org/10.1002/esp.3462>, 2014.
- Lal, D.: Cosmic ray labeling of erosion surfaces: in situ nuclide production rates and erosion models, *Earth and Planetary Science Letters*, 104, 424-439, [https://doi.org/10.1016/0012-821x\(91\)90220-c](https://doi.org/10.1016/0012-821x(91)90220-c), 1991.
- Leonard, J. S. and Whipple, K. X.: Influence of Spatial Rainfall Gradients on River Longitudinal Profiles and the Topographic Expression of Spatially and Temporally Variable Climates in Mountain Landscapes, *Journal of Geophysical Research: Earth Surface*, 126, <https://doi.org/10.1029/2021jf006183>, 2021.



- Litwin, D. G., Malatesta, L. C., and Sklar, L. S.: Hillslope diffusion and channel steepness in landscape evolution models, <https://doi.org/10.5194/egusphere-2024-2418>, 2024.
- Mao, Y., Li, Y., Yan, B., Wang, X., Jia, D., and Chen, Y.: Response of Surface Erosion to Crustal Shortening and its Influence on Tectonic Evolution in Fold-and-Thrust Belts: Implications From Sandbox Modeling on Tectonic
- 345 Geomorphology, Tectonics, 40, <https://doi.org/10.1029/2020tc006515>, 2021.
- Martin, Y.: Modelling hillslope evolution: linear and nonlinear transport relations, Geomorphology, 34, 1-21, [https://doi.org/10.1016/s0169-555x\(99\)00127-0](https://doi.org/10.1016/s0169-555x(99)00127-0), 2000.
- Martinsen, O. J., Sømme, T. O., Thurmond, J. B., Helland-Hansen, W., and Lunt, I.: Source-to-sink systems on passive margins: theory and practice with an example from the Norwegian continental margin, Geological Society, London, Petroleum Geology Conference Series, 7, 913-920, <https://doi.org/10.1144/0070913>, 2022.
- 350 Miller, S. R., Baldwin, S. L., and Fitzgerald, P. G.: Transient fluvial incision and active surface uplift in the Woodlark Rift of eastern Papua New Guinea, Lithosphere, 4, 131-149, <https://doi.org/10.1130/1135.1>, 2012.
- Molin, P., Sembroni, A., Ballato, P., and Faccenna, C.: The uplift of an early stage collisional plateau unraveled by fluvial network analysis and river longitudinal profile inversion: The case of the Eastern Anatolian Plateau, Tectonics, <https://doi.org/10.1029/2022tc007737>, 2023.
- 355 Muzikar, P.: Inferring exposure ages and erosion rates from cosmogenic nuclides: A probabilistic formulation, Quaternary Geochronology, 4, 124-129, <https://doi.org/10.1016/j.quageo.2008.11.005>, 2009.
- Neely, A. B., Bookhagen, B., and Burbank, D. W.: An automated knickzone selection algorithm (KZ-Picker) to analyze transient landscapes: Calibration and validation, Journal of Geophysical Research: Earth Surface, 122, 1236-1261, <https://doi.org/10.1002/2017jf004250>, 2017.
- 360 O'Hara, D., Karlstrom, L., and Roering, J. J.: Distributed landscape response to localized uplift and the fragility of steady states, Earth and Planetary Science Letters, 506, 243-254, <https://doi.org/10.1016/j.epsl.2018.11.006>, 2019.
- Pan, B., Cai, S., and Geng, H.: Numerical simulation of landscape evolution and mountain uplift history constrain—A case study from the youthful stage mountains around the central Hexi Corridor, NE Tibetan Plateau, Science China Earth Sciences, 64, 412-424, <https://doi.org/10.1007/s11430-020-9716-6>, 2021.
- 365 Perron, J. T. and Royden, L.: An integral approach to bedrock river profile analysis, Earth Surface Processes and Landforms, 38, 570-576, <https://doi.org/10.1002/esp.3302>, 2013.
- Perron, J. T., Dietrich, W. E., and Kirchner, J. W.: Controls on the spacing of first-order valleys, Journal of Geophysical Research, 113, <https://doi.org/10.1029/2007jf000977>, 2008.
- 370 Quye-Sawyer, J., Whittaker, A. C., Roberts, G. G., and Rood, D. H.: Fault Throw and Regional Uplift Histories From Drainage Analysis: Evolution of Southern Italy, Tectonics, 40, <https://doi.org/10.1029/2020tc006076>, 2021.
- Robl, J., Hergarten, S., and Prasicek, G.: The topographic state of fluvially conditioned mountain ranges, Earth-Science Reviews, 168, 190-217, <https://doi.org/10.1016/j.earscirev.2017.03.007>, 2017.
- Roering, J. J.: How well can hillslope evolution models "explain" topography? Simulating soil transport and production with
- 375 high-resolution topographic data, Geological Society of America Bulletin, 120, 1248-1262, <https://doi.org/10.1130/b26283.1>, 2008.
- Roering, J. J., Kirchner, J. W., and Dietrich, W. E.: Evidence for nonlinear, diffusive sediment transport on hillslopes and implications for landscape morphology, Water Resources Research, 35, 853-870, <https://doi.org/10.1029/1998wr900090>, 1999.
- 380 Royden, L. and Taylor Perron, J.: Solutions of the stream power equation and application to the evolution of river longitudinal profiles, Journal of Geophysical Research: Earth Surface, 118, 497-518, <https://doi.org/10.1002/jgrf.20031>, 2013.
- Salles, T.: Badlands: A parallel basin and landscape dynamics model, SoftwareX, 5, 195-202, <https://doi.org/10.1016/j.softx.2016.08.005>, 2016.
- 385 Salles, T. and Duclaux, G.: Combined hillslope diffusion and sediment transport simulation applied to landscape dynamics modelling, Earth Surface Processes and Landforms, 40, 823-839, <https://doi.org/10.1002/esp.3674>, 2014.
- Salles, T. and Hardiman, L.: Badlands: An open-source, flexible and parallel framework to study landscape dynamics, Computers & Geosciences, 91, 77-89, <https://doi.org/10.1016/j.cageo.2016.03.011>, 2016.
- Schwanghart, W. and Scherler, D.: TopoToolbox 2 – MATLAB-based software for topographic analysis and modeling in
- 390 Earth surface sciences, Earth Surface Dynamics, 2, 1-7, <https://doi.org/10.5194/esurf-2-1-2014>, 2014.



- Seybold, H., Berghuijs, W. R., Prancevic, J. P., and Kirchner, J. W.: Global dominance of tectonics over climate in shaping river longitudinal profiles, *Nature Geoscience*, 14, 503-507, <https://doi.org/10.1038/s41561-021-00720-5>, 2021.
- Shi, F., Tan, X., Zhou, C., and Liu, Y.: Impact of asymmetric uplift on mountain asymmetry: Analytical solution, numerical modeling, and natural examples, *Geomorphology*, 389, <https://doi.org/10.1016/j.geomorph.2021.107862>, 2021.
- 395 Sklar, L. S. and Dietrich, W. E.: Sediment and rock strength controls on river incision into bedrock, *Geology*, 29, [https://doi.org/10.1130/0091-7613\(2001\)029<1087:Sarsco>2.0.Co;2](https://doi.org/10.1130/0091-7613(2001)029<1087:Sarsco>2.0.Co;2), 2001.
- Smith, A. G. G., Fox, M., Schwanghart, W., and Carter, A.: Comparing methods for calculating channel steepness index, *Earth-Science Reviews*, 227, <https://doi.org/10.1016/j.earscirev.2022.103970>, 2022.
- Sweeney, K. E., Roering, J. J., and Ellis, C.: Experimental evidence for hillslope control of landscape scale, *Science*, 349, 51-53, <https://doi.org/10.1126/science.aab0017>, 2015.
- 400 Tucker, G. E. and Bras, R. L.: Hillslope processes, drainage density, and landscape morphology, *Water Resources Research*, 34, 2751-2764, <https://doi.org/10.1029/98wr01474>, 1998.
- Tucker, G. E. and Hancock, G. R.: Modelling landscape evolution, *Earth Surface Processes and Landforms*, 35, 28-50, <https://doi.org/10.1002/esp.1952>, 2010.
- 405 Whipple, K. X.: Fluvial Landscape Response Time: How Plausible Is Steady-State Denudation?, *American Journal of Science*, 301, 313-325, <https://doi.org/10.2475/ajs.301.4-5.313>, 2001.
- Whipple, K. X.: The influence of climate on the tectonic evolution of mountain belts, *Nature Geoscience*, 2, 97-104, <https://doi.org/10.1038/ngeo413>, 2009.
- Whipple, K. X. and Tucker, G. E.: Dynamics of the stream-power river incision model: Implications for height limits of mountain ranges, landscape response timescales, and research needs, *Journal of Geophysical Research: Solid Earth*, 104, 17661-17674, <https://doi.org/10.1029/1999jb900120>, 1999.
- 410 Whipple, K. X., DiBiase, R. A., and Crosby, B. T.: 9.28 Bedrock Rivers, in: *Treatise on Geomorphology*, edited by: Shroder, J., Wohl, E., Academic Press, San Diego, CA, 550-573, <https://doi.org/10.1016/b978-0-12-374739-6.00254-2>, 2013.
- Whittaker, A. C.: How do landscapes record tectonics and climate?, *Lithosphere*, 4, 160-164, <https://doi.org/10.1130/rl003.1>, 2012.
- 415 Willett, S. D., McCoy, S. W., Perron, J. T., Goren, L., and Chen, C. Y.: Dynamic reorganization of river basins, *Science*, 343, 1248765, <https://doi.org/10.1126/science.1248765>, 2014.
- Wobus, C., Whipple, K. X., Kirby, E., Snyder, N. P., Johnson, J., Spyropoulou, K., Crosby, B., and Sheehan, D.: Tectonics from topography: Procedures, promise, and pitfalls, *Geol Soc Am Spec Pap*, 398, 55-74, [https://doi.org/10.1130/2006.2398\(04\)](https://doi.org/10.1130/2006.2398(04)), 2006a.
- 420 Wobus, C. W., Crosby, B. T., and Whipple, K. X.: Hanging valleys in fluvial systems: Controls on occurrence and implications for landscape evolution, *Journal of Geophysical Research*, 111, <https://doi.org/10.1029/2005jf000406>, 2006b.
- Wobus, C. W., Tucker, G. E., and Anderson, R. S.: Does climate change create distinctive patterns of landscape incision?, *Journal of Geophysical Research: Earth Surface*, 115, <https://doi.org/10.1029/2009jf001562>, 2010.

425